# SEISMIC SCATTERING AND SHALLOW STRUCTURE OF THE MOON IN OCEANUS PROCELLARUM*

ANTON M. DAINTY, M. NAFI TOKSÖZ,
KENNETH R. ANDERSON, and P. JACQUES PINES
*Dept. of Earth and Planetary Sciences, Massachusetts Institute of Technology, Cambridge, Mass., U.S.A.*

and

Y. NAKAMURA, and G. LATHAM
*Marine Biomedical Institute, University of Texas at Galveston, Galveston, Tex., U.S.A.*

(Received 2 February, 1973)

**Abstract.** Long, reverberating trains of seismic waves produced by impacts and moonquakes may be interpreted in terms of scattering in a surface layer overlying a non-scattering elastic medium. Model seismic experiments are used to qualitatively demonstrate the correctness of the interpretation. Three types of seismograms are found, near impact, far impact and moonquake. Only near impact and moonquake seismograms contain independent information. Details are given in the paper of the modelling of the scattering processes by the theory of diffusion.

Interpretation of moonquake and artificial impact seismograms in two frequency bands from the Apollo 12 site indicates that the scattering layer is 25 km thick, with a $Q$ of 5000. The mean distance between scatterers is approximately 5 km at 25 km depth and approximately 2 km at 14 km depth; the density of scatterers appears to be high near the surface, decreasing with depth. This may indicate that the scatterers are associated with cratering, or are cracks that anneal with depth. Most of the scattered energy is in the form of scattered surface waves.

## 1. Introduction

When lunar seismograms were first obtained, one of the most puzzling aspects of them was the extremely long, reverberating train of waves associated with them, and the apparent lack of dispersed, coherent trains of surface waves (Figure 1; Latham *et al.*, 1970a, b). Of the various theories put forward to explain this phenomenon, only one, scattering in a high $Q$ medium, has survived.

A simple experimental setup demonstrates that seismograms such as Figure 1 may be produced by scattering. Figure 2 diagrammatically illustrates a model seismology apparatus used to produce the seismograms shown in Figure 3. Two experiments are illustrated – propagation across a plate with grooves cut half-way through, and propagation along the edge of a plate with holes drilled within a skin depth (for Rayleigh waves) of the edge. The first experiment illustrates a seismogram of the nature of that shown in Figure 1, and the second demonstrates that no coherent trains of surface

* Communication presented at the Lunar Science Institute Conference on 'Geophysical and Geochemical Exploration of the Moon and Planets', January 10–12, 1973.

*The Moon* **9** (1974) 11–29. 

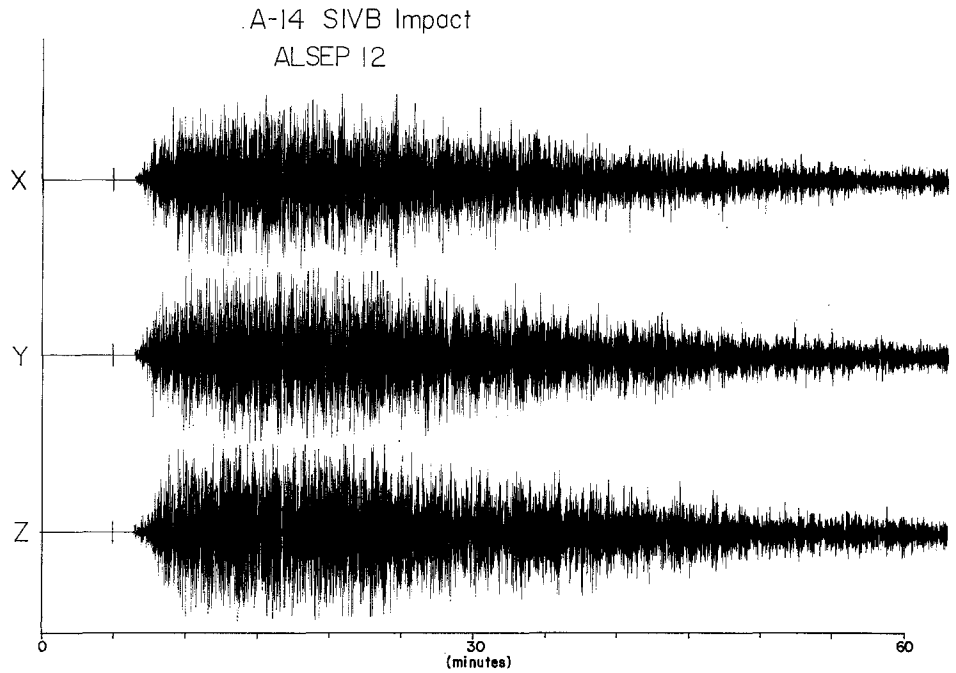


Fig. 1. Seismogram recorded by the Apollo 12 long-period seismometer from the impact of the S4B Saturn booster of Apollo 14. Three components of ground displacement are shown: $X$ is $S-N$ ($S+ve$), $Y$ is $W-E$. The tick marks indicate the impact time. The dominant frequencies present are between 0.5 and 1.0 Hz.

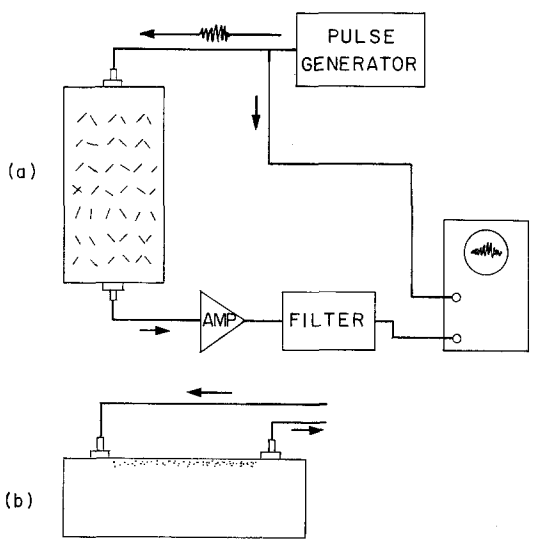


Fig. 2. Model seismology apparatus used to study scattering. In (a), the scatterers in the plate are grooves 0.06″ wide, 1″ long milled half-way through the plate. The center points of the grooves are 0.7″ apart. The plate is 24″ × 9½″ × 0.063″. In (b) holes were drilled part-way through a plate 24″ × 9½″ × × 0.063″ using a ⅛″ drill positioned within a skin depth (for Rayleigh waves) of the edge of the plate. The transducers were 14″ apart. The rest of the experiment was as in (a). Aluminum plates were used, $V_P$—5 mm $\mu s^{-1}$.

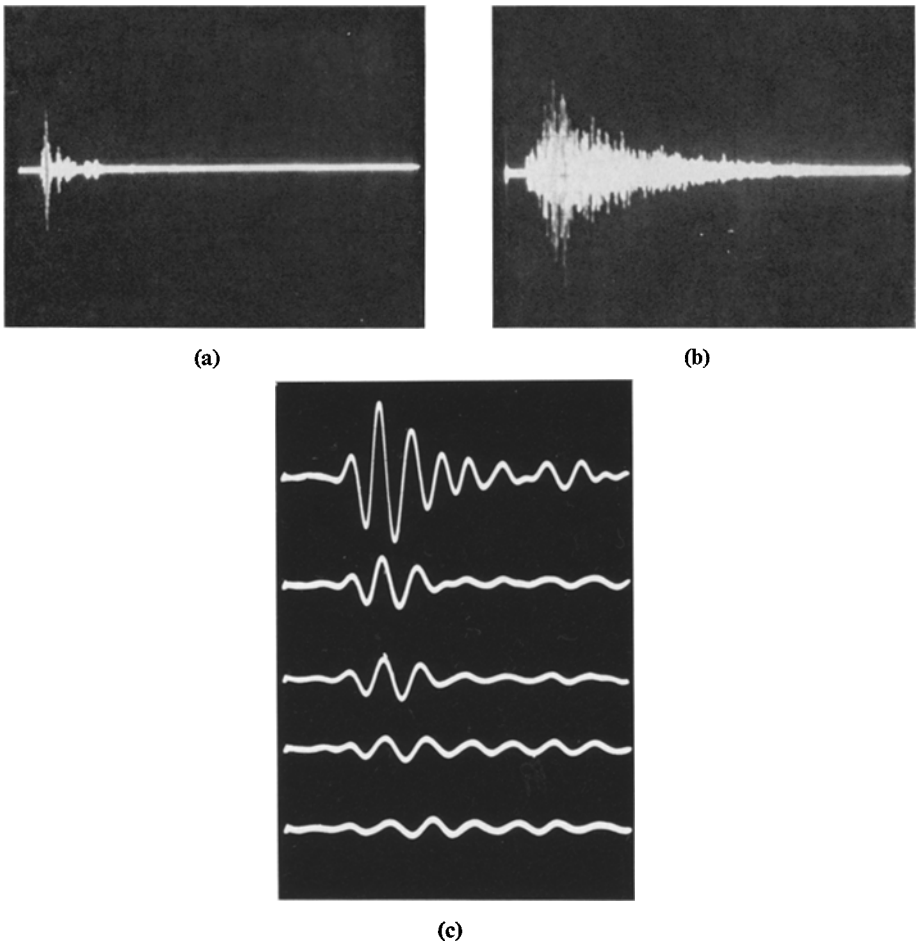


Fig. 3. Seismograms from the model seismology experiment. (a) is from the experiment of Figure 2 (a), but without any grooves in the plate. The seismogram is dominated by coherent reflections. (b) is also from the experiment of Figure 2 (a), but with the grooves cut in the plate as described in the caption of Figure 2. (c) exhibits, from top to bottom, the experiment of Figure 2 (b) with, successively, 0, 2, 4, 6 and 9 holes drilled, with the same vertical sensitivity. In (a) and (b), the time scale is such that the total length of the trace is 2 ms; in (c) it is 40 $\mu$s. The oscillatory character of the signal in (c) is due to ringing in the transducer, not dispersion.

waves will be seen in the presence of scatterers. This study will be expanded to include detailed investigations of the effect of different scatterers and spacing on the form of the seismogram.

There are three variants of the scattering theory of lunar seismograms: surface scattering of surface waves (Nakamura *et al.*, 1970, Berckhemer, 1970; Steg and Klemens, 1970; Latham *et al.*, 1970a, b, c, d; Strobach, 1970), surface scattering of body waves (Gold and Soter, 1970) and scattering of seismic energy in a layer of finite thickness (Latham *et al.*, 1971a, c). Of these, only scattering in a layer of finite thickness can explain all the data and this model will be emphasized here. In this

model there are two channels for seismic energy propagation: through the scattering layer via (mostly) scattered surface waves, and through the underlying medium as compressional or shear body waves.

Scattering of seismic waves has been observed in the earth (Aki, 1969; Wesley, 1965). Warren (1972) has interpreted Aki's data and his own by methods similar to those used here.

## 2. Theory

The model used is that of a surficial scattering layer overlying a medium in which seismic compressional and shear body waves may propagate (Figure 4). Before discussing the details of the scattering process, some general comments will be made on the types of seismograms to be expected. These fall into three groups: close impacts, far impacts, and moonquake seismograms, as illustrated in Figure 4.

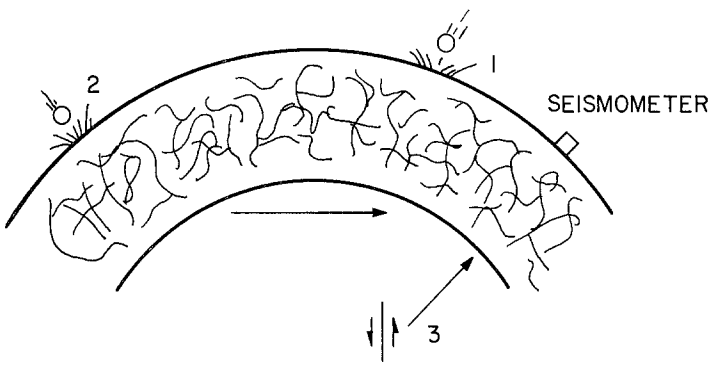


Fig. 4. Model for seismic scattering in the Moon. Energy is intensely scattered in the surface layer, as indicated by curving lines. In the medium below, energy propagates without scattering, as indicated by the arrows. 1 indicates a near impact, 2 a far impact and 3 a moonquake.

Close impact seismograms are produced when the impact is sufficiently close to the seismometer so that energy moves directly through the scattering layer from source to receiver. At a given frequency, the time of arrival of maximum energy, known as the rise time, varies as the square of the range for very close impacts; however, due to the effect of attenuation and scattering of energy out of the layer, for impacts at ranges used in this study the rise time varies as $(\text{range})^{1.3}$. As the impact point moves further from the seismometer, however, a point is reached beyond which seismic body waves may penetrate below the scattering layer after being scattered near the impact, propagate without scattering in the underlying medium, and diffuse up through the scattering layer near the receiver. If this process dominates, and provided the travel time difference between compressional and shear waves in the underlying medium may be ignored, the rise time is independent of range. The non-equality of the travel times of $P$ and $S$ waves leads to a gradual increase in the rise time with range and the eventual separation of the energy envelope (energy as a function of time) of the signal into two distinct envelopes (Nakamura *et al.*, 1973).

Moonquake seismograms are scattered only near the seismometer. This implies a relationship between the energy envelope for moonquakes, $m(t)$, and that for far impacts, $i(t)$, appropriately normalized, of the form

$$i(t) = A(r) \cdot s(t) * m(t), \tag{1}$$

where $A(r)$ is an amplitude function dependent on the velocity structure of the underlying medium, $r$ is range, $s(t)$ is the effect of scattering near the impact and $*$ represents convolution. (1) assumes that the source function is very short in comparison with the time scale of the problem, and that the travel time difference between $P$ and $S$ waves may be ignored. The first assumption is almost certainly true for all impacts, since Toksőz *et al.* (1972c) determined the source function length as approximately 8 s, whereas the time scale of the envelope is tens of minutes. The second assumption is expected to be true for impacts closer than about 400 km.

Using the principal of reciprocity, $s(t) = m(t)$ and (1) becomes

$$i(t) = A \cdot m(t) * m(t).$$

Taking the Fourier transform of both sides and using the convolution theorem, we find that

$$I(w) = A \cdot M^2(w),$$

where capitals indicate the Fourier transform. This leads in turn to

$$M(w) = \sqrt{\frac{I(w)}{A}}. \tag{2}$$

This enables the moonquake envelope to be estimated within a numerical factor from the envelope of far impacts. Whilst no new information is obtained, this is a powerful check on the correctness of the model, and one that is independent of the nature of the scattering process.

The theory used to describe the scattering is diffusion theory. One of the major properties of wave propagation is the directed flow of energy in the direction of propagation. Previous theories of the scattering of seismic waves (see Chernov, 1960, for a review) have assumed this property is mostly preserved, i.e., the scattered field may be considered as a perturbation of the original field. Strong scattering, however, will destroy the directional property of seismic waves. In its place the diffusion hypothesis is proposed, namely that energy flow is in the direction of the gradient of energy, and proportional to that gradient. Nakamura *et al.* (1970) gave a simplified discussion demonstrating why this might be so they suggested that the linear differential equation

$$\frac{\partial e}{\partial t} = \frac{\xi}{4} \nabla^2 e - \frac{w}{Q} e \tag{3}$$

be used to describe the behavior of seismic energy $e$, where the term on the left and the first term on the right form the diffusion equation (Sommerfeld, 1964, pp. 33–34),

and the last term on the right represents linear dissipation. These authors also suggest that the diffusivity $\xi = vl$, where $v$ is the seismic velocity and $l$ is a length characteristic of the distance between scatterers and their scattering efficiency. $Q$ is the quality factor.

The most obvious difficulty in transferring the above theory to the case of an elastic scattering layer with a free surface is the presence of four different forms of elastic seismic energy – compressional waves, shear waves, surface Rayleigh waves and surface Love waves. These four types will have differing seismic velocities and scattering properties, leading to differing diffusivities. However, Figure 1 demonstrates that the four types cannot diffuse separately, since the vertical and horizontal components of displacement do not have differing energy envelopes (at stations other than Apollo 12, the sensitivites of the horizontal components may be greater than the vertical component (Latham *et al.*, 1971a), but the form of the energy envelope is the same for all components). This implies that a radiative equilibrium between the four types of waves dependent only on the properties of the medium is rapidly set up.

In this case, it is not necessary, or possible, to separate seismic energy into the four types. Since all types of waves propagate horizontally, whereas only compressional and shear waves propagate vertically, the effective diffusivities in the horizontal and vertical directions ($\xi_H$ and $\xi_V$, respectively) will be different, with the horizontal diffusivity being larger. The total energy in the scattering layer is mostly in the form of surface waves, which must be converted into body waves to enter the underlying medium. This may be incorporated into the theory by modifying (3) to the anisotropic diffusion equation (Carslaw and Jaeger, 1959, p. 41) with cylindrical symmetry about the source as origin,

$$\frac{\partial e}{\partial t} = \frac{\xi_H}{4}\left(\frac{\partial^2 e}{\partial r^2} + \frac{1}{r}\frac{\partial e}{\partial r}\right) + \frac{\xi_V}{4}\frac{\partial^2 e}{\partial z^2} - \frac{w}{Q}e, \tag{4}$$

where $r$, $z$ are cylindrical polar coordinates, $r$ being the range and $z$ the depth. It should be clearly understood that the use of the anisotropic diffusion equation does not imply that the medium is anisotropic.

The solution of (6) required for this study is that for a point impulse source at the top surface of a layer. No energy may flow across the top surface, and energy is radiated from the bottom surface into the medium below. This problem is solved in an Appendix. For near impacts, the energy envelope $i(t)$ for an impact of unit energy is given by this solution with $z = 0$,

$$i(t) = \frac{4}{\pi \xi_H t h^2} \exp\left(-\frac{r^2}{\xi_H t} - \frac{wt}{Q}\right) \sum_{n=1}^{\infty} \frac{a_n}{2a_n + \sin 2a_n} \exp\left(-\frac{t\xi_V a_n^2}{4h^2}\right), \tag{5}$$

where $h$ = thickness of the layer and the $a_n$ are the positive roots of the equation

$$a \tan(a) = \frac{4hv}{\xi_V}, \tag{6}$$

where $v$ is the seismic velocity in the underlying medium. In (5) the terms before the summation represent two-dimensional diffusion; the rise time may be found by differentiating (5) with respect to time and setting the result equal to zero. The relation rise time varying as $(\text{range})^{1.3}$ mentioned earlier is approximately true within the distance range studied in this paper. The sum represents the modification to two-dimensional diffusion caused by the diffusion of energy out of the layer.

The appropriate solution for the moonquake envelope $m(t)$ assuming an incident seismic wave of unit energy density may be obtained by reciprocity from the solution given in the Appendix. $m(t)$ is the solution given integrated over all $r$ and taken at $z=h$,

$$m(t) = \frac{4}{h} \exp\left(-\frac{w}{Q} t\right) \sum_{n=1}^{\infty} \frac{a_n \cos a_n}{2a_n + \sin 2a_n} \exp\left(-\frac{t\xi_V a_n^2}{4h^2}\right). \tag{7}$$

Finally, it should be noted that considerable caution must be used in relating values of diffusivity obtained from fits of (5) and (7) to the data to the physical properties of the medium. The nature of the scatterers is not known – cracks (Berckhemer, 1970; Warren, 1972) and surface irregularities such as craters (Gold and Soter, 1970; Nakamura *et al.*, 1970; Steg and Klemens, 1970) have been suggested, but all attempts at direct analysis of this problem have been oversimplified. The most promising approach is probably analysis of model seismology experiments, which will be reported at a later time. It should also be noted in any interpretation of the difference between horizontal and vertical diffusivity that the assumption that the elastic energy may be separated into various wave types is only strictly valid for homogeneous, isotropic media (see, for example, Grant and West, 1965, pp. 41–50).

## 3. Analysis of the Data

As demonstrated in the previous section, only two types of data, near impacts and moonquakes, contain independent information. Data of these types from the Apollo 12 station in Oceanus Procellarum have been examined in two frequency bands. The Apollo 12 site was chosen because there is more data available at this site than at any other, and only one site was considered to minimize the effect of possible site differences. The impacts used were a set of artificial impacts of S4B Saturn boosters and LM ascent stages as recorded at the Apollo 12 site. Relevant information is given in Table I; see Latham *et al.* (1973) for further details. Several moonquake envelopes from A1 moonquakes as recorded at the Apollo 12 site were examined (Latham *et al.*, 1971b). All have similar characteristics and an event occurring on July 20, 1970 at 11:44 GMT has been chosen for presentation. The A1 moonquake focus is located at 23° S, 28° W at a depth of 850 km (Latham *et al.*, 1973).

To find the energy envelope of the impacts, successive windows 51.2 s long starting at the impact time of the $z$-component of displacement were Fourier-transformed. The absolute square of the transform was taken and smoothed in the frequency domain

using a three-point Hamming filter, and then integrated over a narrow frequency band around frequency $w$ to obtain the squared vertical displacement in that frequency band. This quantity is $T/(3\varrho w^2)$ times the energy in that frequency band and may be plotted against time to the center of the window as the energy envelope; $\varrho$ is density and $T$ is the window length. A similar procedure was used for moonquakes, starting from the arrival time for $P$ waves.

The data for some artificial impacts are presented in Figures 5 and 6 for the frequency bands 0.42–0.48 Hz and 0.93–1.07 Hz. To ascertain whether any of the impacts in these two figures are near impacts, note that for the low frequency band (Figure 5)

TABLE I

Impact parameters for artificial impacts used in this study. The coordinates of the Apollo 12 station are 3.04S, 23.42W

| Impact | Kinetic Energy (erg) | Date day/mo./yr | Time, GMT hr:min:s | Coordinates (deg) | Distance from Apollo 12 station (km) |
|---|---|---|---|---|---|
| Apollo 12 LM | $3.36 \times 10^{16}$ | 20/11/69 | 22:17:17.7 | 3.94S,21.20W | 73 |
| Apollo 14 S4B | $5.54 \times 10^{17}$ | 4/2/71 | 7:40:55.4 | 8.00S,26.06W | 172 |
| Apollo 14 LM | $3.25 \times 10^{16}$ | 7/2/71 | 0:45:25.7 | 3.42S,19.67W | 114 |
| Apollo 15 S4B | $4.61 \times 10^{17}$ | 29/7/71 | 20:58:42.9 | 1.36S,11.77W | 356 |
| Apollo 16 S4B[a] | $5.00 \times 10^{17}$ | 19/4/72 | $21:02:4 \pm 4$ | $1.3 \pm 0.7$N, $23.8 \pm 0.2$W | 132 |

[a] Parameters for the Apollo 16 S4B impact are estimates, since tracking was lost on this impact (Latham *et al.*, 1973).

the rise time increases with increasing range for distances less than approximately 150 km, but is approximately constant with range thereafter, actually decreasing somewhat at a distance of 172 km. This means that seismic rays from the impact are penetrating below the scattering layer for distances greater than 150 km; from the velocity model of Toksöz *et al.* (1972c) this determines the thickness of the scattering layer at this frequency as 25 km.

For the high frequency band (Figure 6), however, all impacts show an approximately constant rise time with range. This suggests that for this frequency band all impacts are far impacts, leading to a maximum thickness at this frequency of 15 km for the scattering layer. This may be reconciled with the figure of 25 km for the low-frequency band if the density of scatterers is high near the surface and decreases with depth – this is easily understandable if the scatterers are associated with some surface process such as cratering (Nakamura *et al.*, 1970; Steg and Klemens, 1970) or are cracks that tend to anneal with depth (Warren, 1972). The thickness of the scattering layer, and its parameters, are then effective parameters which will depend on the wavelength, i.e., the frequency. The thickness of the scattering layer is probably determined by the point at which the mean distance between scatterers is significantly greater than a wavelength of compressional or shear waves.

An attempt to fit the near impacts in the low frequency band using (5) is shown in Figure 7. The parameters used in the fit are summarized in Table II; the fits presented in this paper represent an attempt to find a single model that represents all the data. The LM12 impact at 73 km is well fitted by the theory. The LM14 impact at 114 km is quite well fitted, but there is an excess of energy at short times. The same phenomenon is seen for the S4B16 impact at 132 km, and there is also an excess of energy at long times. This latter excess is probably due to seismic rays that just penetrate below the scattering layer, making the S4B16 impact transitional between near and far impacts. Also shown is an attempt to fit the S4B14 impact at 172 km as a near impact. It is clearly seen that this cannot be done. The slightly early rise time seen in both Figure 5

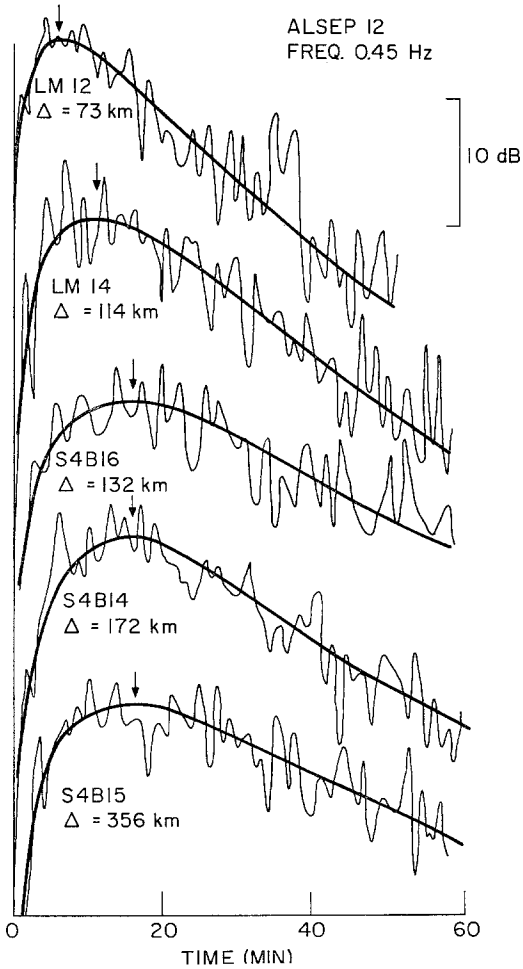


Fig. 5. Suite of artificial impacts. The energy envelopes for the frequency band 0.42–0.48 Hz are shown. The vertical scale is a dB scale with an arbitrary reference level, the envelopes being stacked vertically for purposes of presentation. The heavy lines are smooth curves drawn through the energy envelopes and the arrows indicate the position of the energy maximum.
Table I gives details of the impacts.

TABLE II

Parameters of the scattering layer model

| | | |
|---|---|---|
| Frequency | 0.45 Hz | 1.0 Hz |
| Apparent thickness of scattering layer | 25 km | 14 km |
| Effective horizontal diffusivity | 8 $km^2 s^{-1}$ | not determined |
| Effective vertical diffusivity | 0.9 $km^2 s^{-1}$ | 0.4 $km^2 s^{-1}$ |
| Mean distance between scatterers at base of layer[a] | ~ 5 km | ~ 2 km |
| $Q$ | 5000 | 5000 |
| Elastic propagation velocity in underlying medium | 3.36 km $s^{-1}$ | 3.36 km $s^{-1}$ |

[a] Taken as approximately equal to the wavelength of body waves.

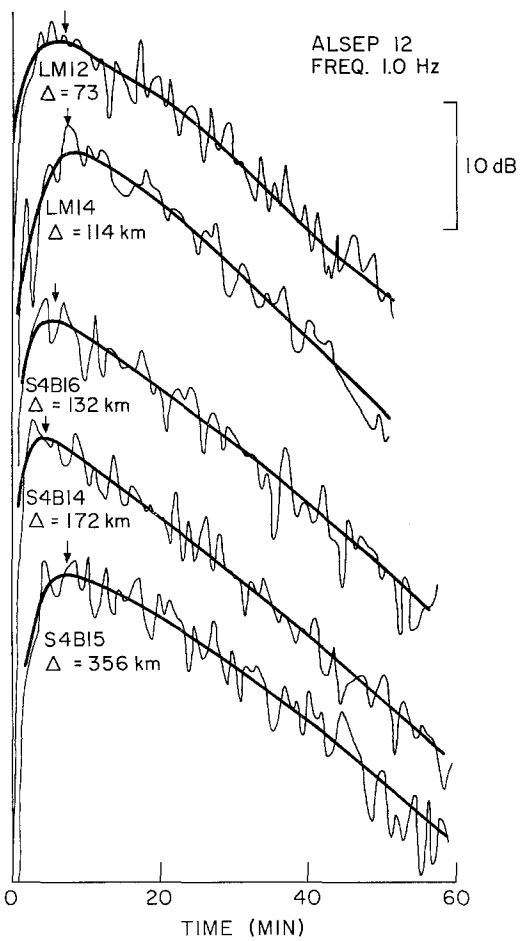


Fig. 6. Energy envelopes for the suite of impacts shown in Figure 5, but for a frequency band 0.93–1.07 Hz. The heavy lines are smooth curves drawn through the energy envelopes, arrows indicate the position of the energy maximum. Table I gives details of the impacts.

and 6 for this impact is probably associated with a cusp in the travel time curve (Toksőz *et al.*, 1972c).

Using (5) and the calibration for the seismograph (Latham *et al.*, 1971a), the total seismic energy generated in the frequency band 0.42–0.48 Hz by the LM12, LM14 and S4B16 impacts may be estimated as $4 \times 10^7$ erg, $3 \times 10$ erg, and $10^{10}$ erg respectively assuming a surface density of 2 gm $cc^{-1}$ (Costes *et al.*, 1971). The ratio of seismic energies for the S4B and LM impacts in this frequency band is approximately 300, as against a ratio of impact energies of 15. This is in agreement with other studies (Latham *et al.*, 1973). The body wave amplitudes between LM and S4B impacts should differ by a factor of about 17, in agreement with the results of Toksőz *et al.* (1972c).

The value 3.36 km $s^{-1}$ used for $v$, the seismic velocity in the underlying medium,

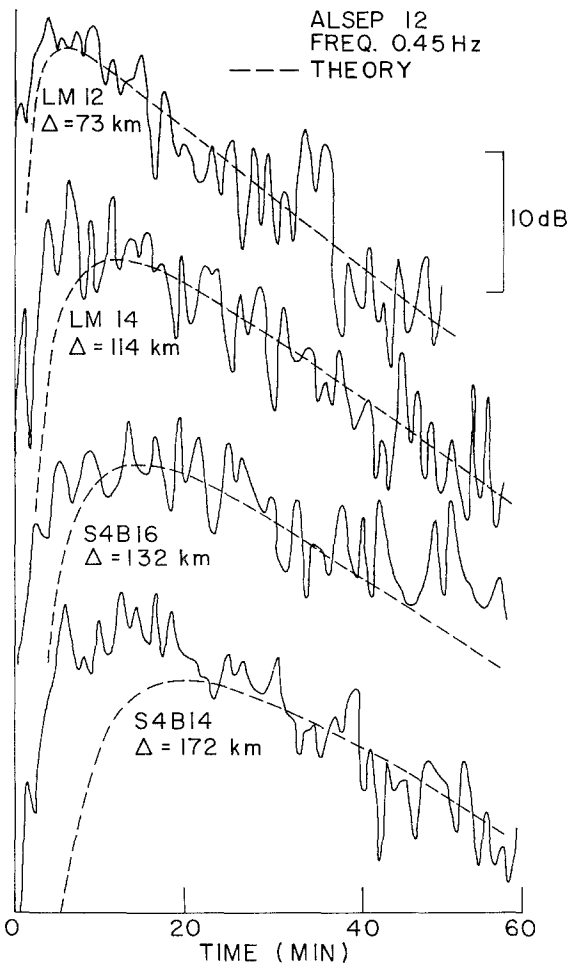


Fig. 7. Comparison of energy envelopes for some impacts with theory for frequencies near 0.45 Hz. The solid line is the observed, the dashed line the theory. Table I gives details of the impacts.

was an average of the $P$ and $S$ velocities at 25 km from Toksöz *et al.* (1972c) averaged over all downward angles of propagation. This leads to a value of $hv/\xi_V$ in (6) of 93. At large values of this parameter, $a_n$ as determined by (6) is not strongly dependent on $hv/\xi_V$. Note that this quantity is approximately the ratio of the time of diffusion through the layer to the time of propagation through a similar distance in the underlying medium.

Data for far impacts and moonquakes in the frequency band 0.42–0.48 Hz is presented in Figure 8. The top part of the figure shows the energy envelope for the S4B15 impact, a typical far impact. The bottom half shows an Al moonquake energy envelope as a light line. The heavy line drawn through the moonquake envelope is derived from the smooth heavy line drawn through the S4B15 envelope by (2); since most of the energy produced at a moonquake focus is known to be in the form of shear waves, this line and the theoretical fit based on (7) (dashed line) have been time shifted by an amount equal to the $P-S$ difference. The vertical component of

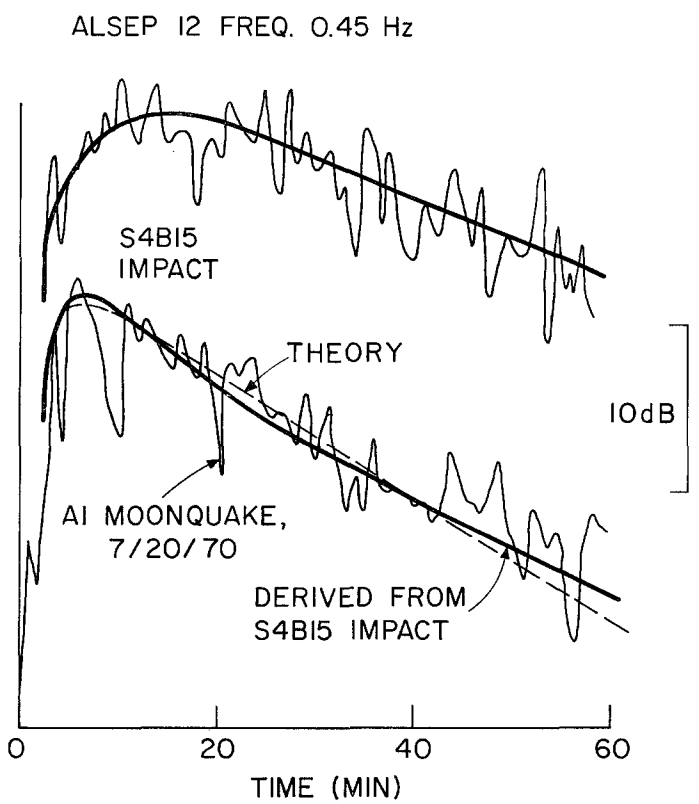


Fig. 8. Comparison of theory and observations for a far impact, S4B15 received at Apollo 12, and a moonquake for frequencies near 0.45 Hz. The top part of the figure shows the S4B15 impact, with a smooth curve (heavy line) drawn through it. The bottom half shows the moonquake envelope (light solid line). The heavy line in the bottom half of the figure has been derived from the heavy line in the top half by (2). The dashed curve is theoretical, and coincides with the heavy solid line where it is not shown.

the moonquake seismogram has been used in Figure 8 – a prominent arrival interpeted as the direct shear wave (Latham *et al.*, 1971b) is present on the horizontal components, thus the vertical component should represent the scattered energy. The parameters used for the theoretical curve are summarized in Table II, and are the same as those used in Figure 7.

Figure 8 shows that the moonquake envelope measured and that derived from a far impact agree well for the frequency range considered. This lends confidence to the model proposed in Figure 4. The fact that the moonquake energy envelope has a finite rise time also indicates that the scatterers are distributed through a layer

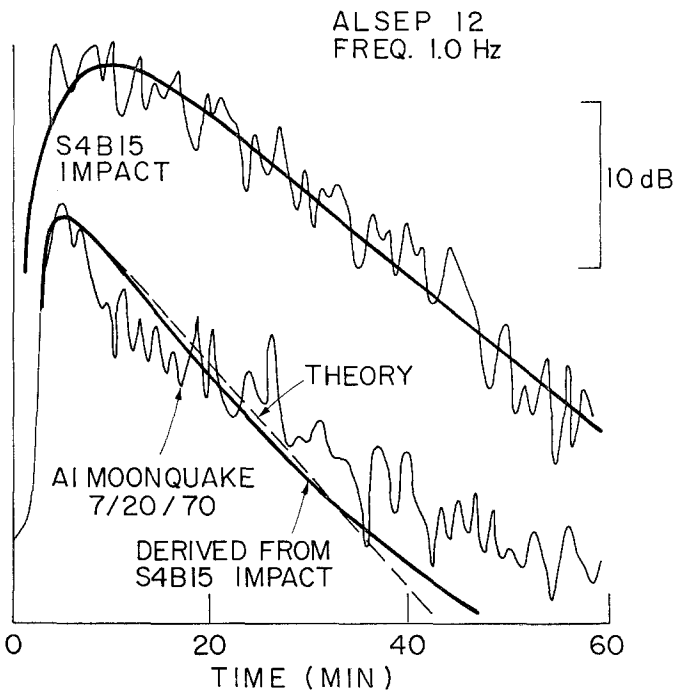


Fig. 9. Comparison of theory and observations for S4B15 and a moonquake for frequencies near 1 Hz. The layout is the same as that of Figure 8.

and are not solely surface scatterers. The incident energy per unit surface area in the frequency band 0.42–0.48 Hz for the shear wave from the Al moonquake shown in Figure 8 is $3.5 \times 10^4$ erg km$^{-2}$ onto the base of the scattering layer.

In the frequency band 0.93–1.07 Hz, there are no near impacts. Thus all parameters of the scattering layer for this frequency band must be derived from the moonquake envelope; it is not possible to determine the horizontal diffusivity. Figure 9 presents the data in a similar fashion to Figure 8. The incident energy per unit surface area in the frequency band 0.93–1.07 Hz for the shear wave is $9.5 \times 10^4$ erg km$^{-2}$. The parameters for the theoretical fit are given in Table II.

## 4. Discussion

The scattering layer model is summarized in Table II. From it, the following conclusions may be tentatively drawn:

(1) The horizontal and vertical diffusivities are different, the horizontal being an order of magnitude larger. This suggests that most of the energy is in the form of scattered surface waves. This does not contradict the lack of observed coherent surface wave trains, since scattering will destroy the coherency. The low value of the vertical diffusivity is probably due to a low proportion of the seismic energy being converted to body waves.

(2) The scattering layer is 25 km thick at 0.45 Hz and 14 km thick at 1.0 Hz. It should be noted from (5) and (7) that strictly speaking only the quantity $h^2/\xi_V$ is determined from the theoretical fits. $\xi_V$ has been assumed inversely proportional to frequency. The density of scatterers is high at the surface and decreases with depth. The effective thickness of the scattering layer is probably controlled by the point at which the mean distance between scatterers becomes larger than the wavelength of seismic energy. This has been indicated in Table II, although caution must be exercised. The decrease in density of scatterers with depth suggests the scatterers are either related to a surface phenomenon, such as cratering, or consist of cracks which anneal with depth. At a depth of 25 km in the models of Toksöz *et al.* (1972c) there is a boundary which may divide shattered from competent rock.

(3) The $Q$ of the scattering layer is 5000. This value has been corrected for scattering of energy out of the layer, unlike previous estimates (Latham *et al.*, 1971a). Whilst the value of $Q$ is somewhat dependent on the model assumed, the presence of seismic energy from an impact over an hour after the impact demands that $Q$ be of this order of magnitude irrespective of the model chosen. The value obtained is considerably higher than those reported for returned lunar rocks (Kanamori *et al.*, 1971; Wang *et al.*, 1971; Warren *et al.*, 1971) or the Active Seismic Experiment (Kovach and Watkins, 1972), which samples the lunar regolith. This point remains unresolved, although the complete absence of water on the moon may be the explanation. Warren (1972) has suggested that the high value of $Q$ indicates scattering from open cracks.

This paper is a first report on a continuing investigation. The work reported here will be extended to other frequencies and other Apollo sites. Two major problems remain unresolved, and are briefly discussed below.

The relationship of the scattered envelope to body waves such as those seen by Toksöz *et al.* (1972a, b, c) is not clear. Body waves are seen clearly as first arrivals on impact seismograms at distances of 100 km and greater, and exhibit consistent relationships with each other and with synthetic seismograms calculated by generalized ray theory, apparently indicating a lack of intense scattering. This may be explained by the steep angle of incidence and resulting short residence time ($\sim$20 s) of such body waves in the scattering layer. These first arrivals are small compared with the rest of the seismograms because of the extremely low velocity of the surface, which allows

only very steeply incident waves to escape from the scattering layer near the impact. A satisfactory explanation for the relation between direct $S$ and the scattered energy for moonquake seismograms has not been ascertained.

As yet, no satisfactory description of the scattering process exists. Warren (1972) has discussed scattering from cracks; Steg and Klemens (1970) examined the scattering of surface waves from surface irregularities. In their comparison with the data, however, they took the mean frequency of the seismic signal as 30 Hz, whereas the true frequency is between 0.5 and 1.0 Hz. Since in their theory the frequency appears as the sixth power, this has a large effect on their comparison. The surface scattering theory of Gold and Soter (1970) cannot explain the finite rise time of moonquakes. The most promising approach to this problem of scattering appears to be model seismology.

## 5. Appendix

The problem of a point impulse of energy situated at the surface of a layer, thickness h, within which anisotropic diffusion is taking place is considered. The surface of the layer is impervious to energy; the bottom surface is in contact with a medium into which energy radiates. Linear dissipation is occurring in the layer. The following reference is used extensively: Carslaw and Jaeger (1959), pp. 18, 41, 372, 373, 491, 696. Explicit reference to this work will not be made hereafter.

The source is taken at the origin of cylindrical polar coordinates $r$, $\theta$, $z$, thus removing any dependence on $\theta$. The diffusing medium has principal diffusivities $\xi_1/4$, $\xi_1/4$, $\xi_3/4$ in the $r$, $\theta$, $z$ directions respectively. The boundary condition at $z=0$ is $\partial e/\partial z=0$. To find the boundary condition at $z=h$, consider a pill box whose vertical extent is negligible compared to its horizal extent, with one horizontal face of area $\Delta S$ in the boundary and the other just above the boundary. Then the flux of energy into the top surface of the pill box is $(-\xi_3/4)\,(\partial e/\partial z)\,\Delta S$. At the bottom of the pill box, energy is carried away by wave propagation. The flux of energy in such a case is $v\mathbf{n}$.e, where $\mathbf{n}$ is a unit vector in the direction of the wave normal and $v$ is the wave velocity of the medium (Morse and Feshbach, 1953, p. 151). In this case, there are two wave velocities corresponding to compressional and shear waves, and the direction of propagation is presumably random into the medium. It will be assumed that the flux of energy in the vertical direction may nonetheless be written as $ve$, where $v$ is of the same order of magnitude as the wave velocities. Remembering that the vertical extent of the pill box is negligible, and applying the conservation of energy to the pill box, the boundary condition at $z=h$ may be written as $-(\xi_3/4)\,(\partial e/\partial z)=ve$, or $(\xi_3/4)\,(\partial e/\partial z)+ve=0$.

The layer has a quality factor $Q$ and the frequency of the energy is taken as $w$. The solution in the diffusing layer may be written as

$$e(r, z, t, w) = g(r, z, t, w) + f(r, z, t, w),$$

where $g$ is the Green's function for the infinite medium, and $f$ is a solution of the

homogeneous equation

$$\frac{\xi_1}{4}\left(\frac{\partial^2 f}{\partial r^2}+\frac{1}{r}\frac{\partial f}{\partial r}\right)+\frac{\xi_3}{4}\frac{\partial^2 f}{\partial z^2}-\frac{w}{Q}f-\frac{\partial f}{\partial t}=0, \tag{A-1}$$

chosen so that $e$ satisfies the boundary conditions. In the analysis following the notation $L(e)=E$, $L(g)=G$, $L(f)=\mathrm{F}$ will be used, where $L(\ )$ is the Laplacian operator.

The function $g(r,z,t,w)$ is given by

$$g(r,z,t,w)=\frac{2e_0}{(\pi^3 t^3 \xi_1^2 \xi_3)^{1/2}}\exp\left(-\frac{r^2}{\xi_1 t}-\frac{z^2}{\xi_3 t}-\frac{w}{Q}t\right) \tag{A-2}$$

and

$$G(r,z,p,w)=\frac{e_0}{\sqrt{r^2/\xi_1+z^2/\xi_3}}\left\{\frac{2}{\pi\xi_1\sqrt{\xi_3}}\right\}\times \exp\left(2\sqrt{p+w/Q}\sqrt{r^2/\xi_1+z^2/\xi_3}\right).$$

Using the identity

$$\frac{\exp(-q\sqrt{x^2+y^2})}{\sqrt{x^2+y^2}}=\int_0^\infty J_0(kx)\exp(-\eta y)\,(k/\eta)\,\mathrm{d}k,$$

where $J_0(u)=$ Bessel function of zero-th order and first kind,

$$\eta=\sqrt{k^2+q^2}, \quad \text{and} \quad y>0,$$

$$G=\frac{2e_0}{\pi\xi_1\sqrt{\xi_3}}\int_0^\infty J_0\left(k\frac{r}{\sqrt{\xi_1}}\right)\exp\left(-\eta\frac{z}{\sqrt{\xi_3}}\right)\frac{k}{\eta}\,\mathrm{d}k; \tag{A-3}$$

with $\eta=\sqrt{k^2+4(p+w/Q)}$ ($z$ is taken positive downwards). Note that (A-3) apparently does not obey the boundary condition at $z=0$. This is because only the soluton for $z>0$ has been written, i.e., only the solution within the layer. At $z=0$, there is a discontinuity in $G$ due to the source – noting that (A-2) *does* obey the boundary conditions at $z=0$, (A-3) will be considered to obey it too. Thus when $f(r,z,,t,w)$ is found, it must obey the boundary condition at $z=0$. To find $f$, Laplace transform ($A$-1) to obtain

$$\xi_1\left(\frac{\partial^2 F}{\partial r^2}+\frac{1}{r}\frac{\partial F}{\partial r}\right)+\xi_3\frac{\partial^2 F}{\partial z^2}-4(p+w/Q)F=0.$$

A solution which obeys the boundary condition at $z=0$ is

$$F=\frac{2e_0 A}{\pi\xi_1\sqrt{\xi_3}}\int_0^\infty\left[\exp\left(-\eta\frac{z}{\sqrt{\xi_3}}\right)+\exp\left(\eta\frac{z}{\sqrt{\xi_3}}\right)\right]J_0\left(k\frac{r}{\sqrt{\xi_1}}\right)\frac{k}{\eta}\,\mathrm{d}k,$$

where $A$ is constant.

Then

$$E = \frac{2e_0}{\pi\xi_1\sqrt{\xi_3}} \int_0^\infty \left[ (1+A)\exp\left(-\eta\frac{z}{\sqrt{\xi_3}}\right) + A\exp\left(\eta\frac{z}{\sqrt{\xi_3}}\right)\right] \times \\ \times J_0\left(k\frac{r}{\sqrt{\xi_1}}\right)\frac{k}{\eta}\,\mathrm{d}k,$$

where $A$ is to be determined from the boundary condition at $z=h$. After some work, we find that

$$E = \frac{2}{\pi\xi_1\sqrt{\xi_3}} \int_0^\infty \frac{\cosh\left[(z+h)\frac{\eta}{\sqrt{\xi_3}}\right] + \frac{4v}{\eta\sqrt{\xi_3}}\sinh\left[(z+h)\frac{\eta}{\sqrt{\xi_3}}\right]}{\sinh\left(\frac{\eta}{\sqrt{\xi_3}}h\right) + \frac{4v}{\eta\sqrt{\xi_3}}\cosh\left(\frac{\eta}{\sqrt{\xi_3}}h\right)} \times \\ \times J_0\left(k\frac{r}{\sqrt{\xi_1}}\right)\frac{k}{\eta}\,\mathrm{d}k, \tag{A-4}$$

where $e_0$, the energy of the impulse, has been set equal to unity. To evaluate this integral, note that it may be written as

$$E = \frac{2}{\pi^2 i\xi_1\sqrt{\xi_3}} \int_{-i\infty}^{i\infty} \frac{\cosh\left[(z+h)\frac{\zeta}{\sqrt{\xi_3}}\right] + \frac{4v}{\zeta\sqrt{\xi_3}}\sinh\left[(z+h)\frac{\zeta}{\sqrt{\xi_3}}\right]}{\sinh\left[\frac{\zeta}{\sqrt{\xi_3}}h\right] + \frac{4v}{\zeta\sqrt{\xi_3}}\cosh\left[\frac{\zeta}{\sqrt{\xi_3}}h\right]} \times \\ \times K_0\left(k\frac{r}{\sqrt{\xi_1}}\right)\frac{k}{\zeta}\,\mathrm{d}k,$$

where $K_0(u)$ is a modified Bessel function of the zeroth order, and $\zeta = \sqrt{4(p+w/Q)-k^2}$. A discussion of the properties of $K_0(u)$ may be found in Abramowitz and Stegun (1965).

This integral may be evaluated by completing the contour in the right half-plane of $k$. Whilst $K_0(u)\to\infty$ as $u\to 0$, it has opposing signs on either side of $u=0$, and the resulting improper integrals cancel. There is a branch cut along the negative real axis of $k$ from $k=0$ to $-\infty$ due to $K_0[k(r/\sqrt{\xi_1})]$ but this is not included in the contour. There is no branch cut due to the radical $\zeta$ since the integrand is even with respect to it. This leaves only the poles of the integrand given by

$$\zeta\sinh\left(\frac{\zeta}{\sqrt{\xi_3}}h\right) + \frac{4v}{\sqrt{\xi_3}}\cosh\left(\frac{\zeta}{\sqrt{\xi_3}}h\right) = 0.$$

If we write $\zeta h/\sqrt{\xi_3} = ia$, this becomes

$$a\tan(a) = \frac{4hv}{\xi_3}. \tag{A-5}$$

There are an infinite number of roots $a_n$, all real; if $a_n$ is a root, $-a_n$ is a root. Since all quantities of interest will turn out to be even with respect to $a_n$, only the positive roots need be considered. The poles in the $k$-plane are given by

$$k = \pm\left[\frac{a_n^2\xi_3}{h^2} + 4\left(p + w/Q\right)\right]$$

and are real. Only the positive roots are included in the contour, and the integral (A-4) may finally be evaluated as $-2\pi i$ (sum of residues). (The minus sign is used because the contour is traversed clockwise rather than counterclockwise.) This evaluation leads to

$$E = \frac{8}{\pi\xi_1 h}\sum_{n=1}^{\infty}\frac{a_n\cos\left(a_n\dfrac{z}{h}\right)}{2a_n + \sin 2a_n}K_0\left(\frac{r}{\sqrt{\xi_1}}\sqrt{\xi_3 a_n^2/h^2 + 4(p + w/Q)}\right).$$

Then

$$e(r, z, t, w) = L^{-1}(E) =$$

$$= \frac{4}{\pi\xi_1 th}\exp\left(-\frac{r^2}{\xi_1 t} - \frac{wt}{Q}\right)\sum_{n=1}^{\infty}\frac{a_n\cos\left(a_n\dfrac{z}{h}\right)}{2a_n + \sin 2a_n}\exp\left[-\frac{t\xi_3 a_n^2}{4h^2}\right].$$

## Acknowledgments

We are grateful to Drs K. Aki, J. Dorman, F. Duennebier, D. Lammlein and S. Solomon for many informative discussions. Our special thanks to Mr S. Stein for help in processing the data. This research was supported by NASA contracts NAS9-12334 and NAS9-5957.

## References

Abramowitz, M. and Stegun, I. A.: 1965, *Handbook of Mathematical Functions*, Dover Publications, Inc.

Aki, K.: 1969, *J. Geophys. Res.* **74**, 615–631.

Berckhemer, H.: 1970, *Z. Geophys.* **36**, 523–529.

Carslaw, H. S. and Jaeger, J. C.: 1959, *Conduction of Heat in Solids*, 2nd ed., Oxford University Press.

Chernov, L. A.: 1960, *Wave Propagation in a Random Medium*, McGraw-Hill, Inc.

Costes, N. C., Cohron, G. T., and Moss, D. C.: 1971, *Proc. 2nd Lunar Sci. Conf.* **3**, 1973–1987.

Gold, T. and Soter, S.: 1970, *Science* **169**, 1071–1075.

Grant, F. S. and West, G. F.: 1965, *Interpretation Theory in Applied Geophysics*, McGraw-Hill, Inc.

Kanamori, H., Mizutani, H., and Hamano, Y.: 1971, *Proc. 2nd Lunar Sci. Conf.* **3**, 2323–2326.

Kovach, R. L. and Watkins, J. S.: 1972, *Rev. Abs. 3rd Lunar Sci. Conf.*, 461–462.

Latham, G. V., Ewing, M., Press, F., Sutton, G., Dorman, J., Nakamura, Y., Toksöz, N., Wiggins, R., Derr, J., and Duennebier, F.: 1970a, *Science* **167**, 455–457.

Latham, G. V., Ewing, M., Press, F., Sutton, G., Dorman, J., Nakamura, Y., Toksőz, N., Wiggins, R., Derr, J., and Duennebier, F.: 1970b, *Proc. Apollo 11 Lunar Sci. Conf.* **3**, 2309–2320.

Latham, G. V., Ewing, M., Press, F., Sutton, G., Dorman, J., Nakamura, Y., Toksőz, N., Wiggins, R., and Kovach, R.: 1970c, *Apollo 12 Preliminary Science Report, NASA SP-235*, 39–53.

Latham, G., Ewing, M., Dorman, J., Press, F., Toksőz, N., Sutton, G., Meissner, R., Duennebier, F., Nakamura, Y., Kovach, R., and Yates, M.: 1970d, *Science* **170**, 620–626.

Latham, G. V., Ewing, M., Press, F., Sutton, G., Dorman, J., Nakamura, Y., Toksöz, N., Duennebier, F., and Lammlein, D.: 1971a, *Apollo 14 Preliminary Science Report, NASA SP-272*, 133–161.

Latham, G. V., Ewing, M., Dorman, J., Lammlein, D., Press, F., Toksöz, N., Sutton, G., Duennebier, F., and Nakamura, Y.: 1971b, *Science* **174**, 687–692.

Latham, G. V., Ewing, M., Press, F., Sutton, G., Dorman, J., Nakamura, Y., Toksőz, N., Lammlein, D., and Duennebier, F.: 1971c, *Apollo 15 Preliminary Science Report, NASA SP-289*, 8-1–8-25.

Latham, G., Ewing, M., Press, F., Sutton, G., Dorman, J., Nakamura, Y., Toksöz, N., Lammlein, D., and Duennebier, F.: 1973, *Apollo 16 Preliminary Science Report, NASA Special Publication,* in press.

Morse, P. M. and Feshbach, H.: 1953, *Methods of Theoretical Physics*, McGraw-Hill, Inc.

Nakamura, Y., Latham, G. V., Ewing, M., and Dorman, J.: 1970, *EOS* **51**, 776 (Abs.).

Nakamura, Y., Lammlein, D., Latham, G., Ewing, M., and Dorman, J.: 1973, *The Moon*, this issue.

Sommerfeld, A.: 1964, *Partial Differential Equations in Physics*, Academic Press.

Steg, R. G. and Klemens, P. G.: 1970, *Phys. Rev. Letters* **24**, 381–383.

Strobach, K.: 1970, *Z. Geophys.* **36**, 643–645.

Toksöz, M. N., Press, F., Anderson, K., Dainty, A., Latham, G., Ewing, M., Dorman, J., Lammlein, D., Nakamura, Y., Sutton, G., and Duennebier, F.: 1972a, *The Moon* **4**, 490–504.

Toksöz, M. N., Press, F., Anderson, K., Dainty, A., Latham, G., Ewing, M., Dorman, J., Lammlein, D., Sutton, G., Duennebier, F., and Nakamura, Y.: 1972b, *Science* **176**, 1012–1016.

Toksöz, M. N., Press, F., Dainty, A., Anderson, K., Latham, G., Ewing, M., Dorman, J., Lammlein, D., Sutton, G., and Duennebier, F.: 1972c, *Proc. 3rd Lunar Sci. Conf.* **3**, 2527–2544.

Wang, H., Todd, T., Weidner, D., and Simmons, G.: 1971, *Proc. 2nd Lunar Sci. Conf.* **3**, 2327–2336.

Warren, N.: 1972, *The Moon* **4**, 430–441.

Warren, N., Schreiber, E., Scholz, C., Morrison, J. A., Norton, P. R., Kumazawa, M., and Anderson, O. L.: 1971, *Proc. 2nd Lunar Sci. Conf.* **3**, 2345–2360.

Wesley, J. P.: 1965, *J. Geophys. Res.* **70**, 5099–5106.